IMM-UGHF-NJ for Continuous Wave Bistatic Sonar Tracking with Propagation Delay

Rong Yang, Yaakov Bar-Shalom, Claude Jauffret, Annie-Claude Perez, Gee Wah Ng

IMM-UGHF-NJ for Continuous Wave Bistatic Sonar Tracking with Propagation Delay

Rong Yang
Asian Society of Information Exploitation, Singapore
yrfio@yahoo.com

Yaakov Bar-Shalom
University of Connecticut, Storrs, CT 06269, USA
ybs@engr.uconn.edu

Claude Jauffret, Annie-Claude Pérez
University of Toulon, IM2NP, UMR7334, CS 60584, 83041 TOULON Cedex, France
jauffret@univ-tln.fr
annie-claude.perez@univ-tln.fr

Gee Wah Ng
National University of Singapore
4, Engineering Drive 3, Singapore 117583
mpengw@nus.edu.sg

***Abstract*—Acoustic propagation delay has not been investigated for a continuous wave multistatic sonar tracking system except for the recent study conducted by Jauffret et al. [4], which estimates the trajectory of a constant velocity target. The results showed that the estimate bias caused by the propagation delay is not negligible, especially for a bistatic system. This paper develops an interacting multiple model unscented Gauss-Helmert filter with numerical Jacobian (IMM-UGHF-NJ) to track a maneuvering target with propagation delay using a bistatic sonar system. The IMM-UGHF-NJ can overcome the two tracking challenges introduced by the delay, namely, implicit state transition model and lack of analytical expression of the Doppler shifted frequency in the measurement model. Simulation tests have been conducted, and the results show that the IMM-UGHF-NJ can reduce the estimation error significantly, especially for fast moving targets.**

***Keywords*—Propagation delay, continuous active sonar, unscented Gauss-Helmert filter, numerical Jacobian.**

I. Introduction

Continuous active sonar (CAS), also known as high duty cycle (HDC) sonar, with multistatic setup has attracted the research interest recently. In such a system, the signal is transmitted almost in a full duty cycle. Compared to the commonly used pulse active sonar (PAS) system, which transmits only a short pulse in a cycle, the CAS system has continuous detection capability, and is less disturbing to underwater fauna through using a low intensity signal.

There are two main types of CAS systems according to the signal waveforms transmitted, namely, frequency modulated (FM) waveforms and continuous constant frequency waveforms (CW). The FM-CAS can provide good target bistatic range information, whereas the CW-CAS has good Doppler shifted frequency measurement (linked to target range rate). The FM-CAS needs to separate indirect path signal from strong direct path signal via methods, such as m-sequence modulation [2] and Dopplergram [8]. The FM-CAS has a frequency bandwidth limitation issue in multistatic system, as broadband waveforms are transmitted repeatedly [3]. The CW-CAS transmits a single fixed frequency waveform, so that it has no frequency bandwidth limitation problem as the FM-CAS. However, due to lack of range information, the observability of a target trajectory in CW-CAS is not as good as FM-CAS, especially for bistatic (a single transmitter-receiver pair) system.

We focus on target tracking using CW-CAS in this paper. A few approaches on this problem have been proposed in literature before. A Gaussian mixture probability hypothesis density (GMPHD) filter was developed in [3]. It tracks multiple constant velocity (CV) targets using bearings and Doppler frequencies detected by multistatic CW-CAS. Results show that CV targets can be tracked using more than two transmitter-receiver pairs when target range is not available. This research does not take signal propagation delay into consideration. The effect of propagation delay of CW-CAS has been studied in [4] recently. An exact Doppler frequency model with propagation delay was proposed. and a maximum likelihood (ML) estimator based on this model was developed to perform batch estimation for a CV target. The simulation results showed that the estimation bias induced by the propagation delay is not negligible, especially for a bistatic system.

In this paper, the propagation delay problem raised in [4] is studied further. We extend the target CV trajectory estimation using a batch parameter estimation technique to the dynamic recursive estimation, which can handle not only CV motion but also maneuvering motion. This extension faces two challenges. Firstly, the "target time" t_k and target position (x_k,y_k) in the state [defined later in (1) and (2)] are highly correlated after propagation delay is introduced. This leads to a state transition equation in an implicit form instead of the commonly used explicit form in [9][10]. Secondly, the Doppler shifted frequency (one of the measurements) does not have an analytical expression in terms of the target state. This is because the Doppler frequency is a function of the bistatic range rate which cannot be described analytically after propagation delay is introduced. Details will be given later in Section II-B. The two challenges mentioned above were overcome in [4] through solving a 2nd order polynomial equation for CV target. However, the approach in [4] cannot be applied to a maneuvering target with coordinated turn (CT) motion, and the new approach in this paper will be shown to handle this.

A dynamic estimation problem uses two basic models,

Yaakov Bar-Shalom was supported by ARO Grant W911NF-10-1-0369.

namely, the state transition model and the measurement model. The state transition model describes the evolution of the target state with time, and it is (in most cases) an explicit expression of the state at the current time in terms of the state at the previous time. The measurement model relates the measurement to the state. The two challenges of the dynamic estimation problem considered in this paper are: (i) the implicit state transition model; (ii) the lack of an analytical measurement model. These make this problem impossible to solve using existing filters.

We will develop an interacting multiple model unscented Gauss-Helmert filter with numerical Jacobian (IMM-UGHF-NJ) to cope with the challenges mentioned above. The IMM [1] is a well known hybrid algorithm to handle motion model uncertainty in maneuvering target tracking. The UGHF [9][10] is a recently developed algorithm for bearings-only tracking (BOT) with implicit state transition model introduced by the acoustic propagation delay. It can be applied to our problem. For the measurement model without analytical form, the NJ (numerical Jacobian) algorithm, which computes the Jacobian numerically, can be utilized [6][11][7]. The Doppler shifted frequency is a function of the bistatic range rate, $\dot{r}$, which has no analytical form due to the unknown time delay. We can compute $\dot{r}$ (derivative of range r) using the NJ.

The structure of the rest of paper is as follows. Section II formulates the problem. Section III presents the IMM-UGHF-NJ. Simulation results and conclusions are in Sections IV and V, respectively.

II. Problem Formulation

The problem is illustrated in Fig. 1. At dynamic estimation cycle k, the transmitter emits a CW signal with constant frequency f^{T} at time t_k^{T}, and the receiver receives the Doppler shifted frequency f^{R} at time t_k^{R} via the target reflection at time t_k. We assume the transmitter and receiver are stationary and located at $(x^{\mathrm{T}},y^{\mathrm{T}})$ and $(x^{\mathrm{R}},y^{\mathrm{R}})$, respectively. The target is moving and its location is $[x(t_k),y(t_k)]$ at reflection time t_k. The ranges between the target at t_k to the transmitter and the receiver are r_k^{T} and r_k^{R}, respectively.

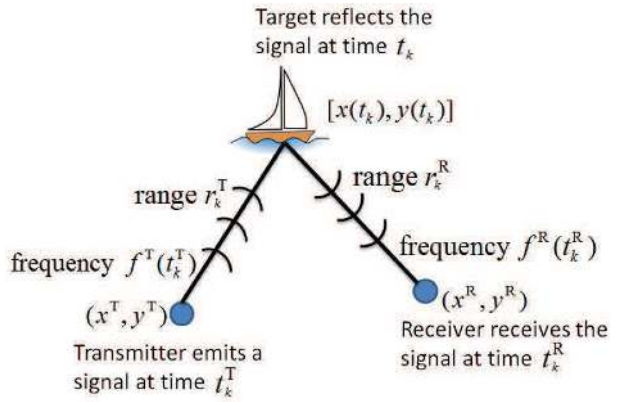

Fig. 1. Signal transmission of CW bistatic sonar.

The target states to be estimated for the CV and CT models at time t_k are

$$\mathbf{x}^{\mathrm{CV}}(t_k) = [x(t_k) \;\; y(t_k) \;\; \dot{x}(t_k) \;\; \dot{y}(t_k) \;\; t_k]' \quad (1)$$

$$\mathbf{x}^{\mathrm{CT}}(t_k) = [x(t_k) \;\; y(t_k) \;\; \dot{x}(t_k) \;\; \dot{y}(t_k) \;\; \omega(t_k) \;\; t_k]' \quad (2)$$

where x, y, $\dot{x}$ and $\dot{y}$ are the target positions and velocities in the x and y coordinates, respectively, ω is the target turn rate, and t_k is the target time (or reflection time) corresponding to the emission time t_k^{T} and the reception time t_k^{R} of the transmitter and receiver, respectively. The measurement vector at time t_k^{R} is

$$\mathbf{z}(t_k^{\mathrm{R}}) = [b(t_k^{\mathrm{R}}) \;\; f^{\mathrm{R}}(t_k^{\mathrm{R}})]' \quad (3)$$

where b is the target bearing from the receiver at time t_k^{R} to the target at time t_k, measured clockwise from True North, and f^{R} is the Doppler shifted frequency at the receiver.

A. State transition models

The state transition model describes the evolution of the target state with time. For a generic discrete problem, it is an explicit form given by

$$\mathbf{x}(t_k) = \mathbf{f}[\mathbf{x}(t_{k-1})] + \Gamma\mathbf{v}(t_{k-1}) \quad (4)$$

where k is the discrete estimation cycle index, $\mathbf{v}(t_{k-1})$ is the process noise, and Γ is the process noise gain. However, there

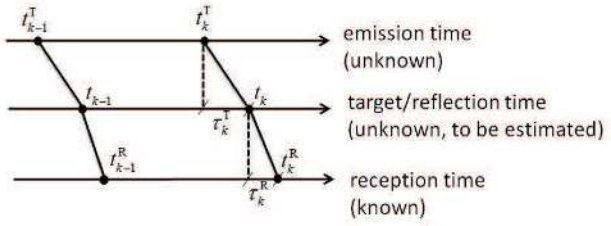

Fig. 2. Time sequences of continuous wave bistatic sonar.

is no explicit state transition model for our problem. It can be seen from Fig. 2 that the target time, t_k, is unknown due to the unknown propagation delay τ^{R}. There is an implicit constraint between the known t_k^{R} and unknown t_k given by

$$t_k = t_k^{\mathrm{R}} - \tau_k^{\mathrm{R}} \quad (5)$$

where

$$\tau_k^{\mathrm{R}} = \frac{\sqrt{[x(t_k) - x^{\mathrm{R}}]^2 + [y(t_k) - y^{\mathrm{R}}]^2}}{c^{\mathrm{P}}} \quad (6)$$

and c^{P} is the signal propagation speed in the medium. It can be seen that t_k is on the both sides of the constraint equation (5), since $x(t_k)$ and $y(t_k)$ are functions of t_k. It is difficult to obtain an explicit express of t_k. This leads to use a Gauss-Helmert (GH) state transition model, which describes an implicit constraint systemically [9][10]. The GH model is given by

$$\mathbf{g}[\mathbf{x}(t_k), \mathbf{x}(t_{k-1})] + \Gamma\mathbf{v}(t_{k-1}) = \mathbf{0} \quad (7)$$

The GH models for the CV motion[1] and CT motion are given next.

[1]Although an explicit state transition model for the CV motion can be obtained through solving a 2nd order polynomial equation [4], the GH model is a systematical way which is suitable for both CV and CT motions.

1) Constant velocity Gauss-Helmert model

The GH model for CV motion is given by

$$\mathbf{g}^{\mathrm{CV}}\left[\mathbf{x}^{\mathrm{CV}}(t_k), \mathbf{x}^{\mathrm{CV}}(t_{k-1})\right] + \Gamma^{\mathrm{CV}}\mathbf{v}^{\mathrm{CV}}(t_{k-1}) = \mathbf{0}_5 \quad (8)$$

where $\mathbf{g}^{\mathrm{CV}}[\cdot]$ is the implicit GH state transition function, which combines the CV motion constraints and the delay constraint between $\mathbf{x}(t_k)$ and $\mathbf{x}(t_{k-1})$. It is given by

$$\mathbf{g}^{\mathrm{CV}}(\cdot) = \left[g_1^{\mathrm{CV}}(\cdot)\ g_2^{\mathrm{CV}}(\cdot)\ g_3^{\mathrm{CV}}(\cdot)\ g_4^{\mathrm{CV}}(\cdot)\ g_5^{\mathrm{CV}}(\cdot)\right]' \quad (9)$$

where

$$\begin{aligned} g_1^{\mathrm{CV}}(\cdot) &= x(t_k) - [x(t_{k-1}) + \dot{x}(t_{k-1})\Delta_k] && (10)\\ g_2^{\mathrm{CV}}(\cdot) &= y(t_k) - [y(t_{k-1}) + \dot{y}(t_{k-1})\Delta_k] && (11)\\ g_3^{\mathrm{CV}}(\cdot) &= \dot{x}(t_k) - \dot{x}(t_{k-1}) && (12)\\ g_4^{\mathrm{CV}}(\cdot) &= \dot{y}(t_k) - \dot{y}(t_{k-1}) && (13)\\ g_5^{\mathrm{CV}}(\cdot) &= t_k - (t_k^{\mathrm{R}} - \tau_k^{\mathrm{R}}) && (14) \end{aligned}$$

with τ_k^{R} given in (6) and

$$\Delta_k = t_k - t_{k-1} \quad (15)$$

Based on the discrete white noise acceleration (WNA) model [1], the gain matrix Γ^{CV} and the zero-mean white Gaussian process noise $\mathbf{v}^{\mathrm{CV}}$ in (8) compensate for small accelerations and the uncertainty of the sound speed. The noise gain matrix Γ^{CV} is given by

$$\Gamma^{\mathrm{CV}} = \begin{bmatrix} \frac{1}{2}(\Delta_k)^2 & 0 & 0 \\ 0 & \frac{1}{2}(\Delta_k)^2 & 0 \\ \Delta_k & 0 & 0 \\ 0 & \Delta_k & 0 \\ 0 & 0 & 1 \end{bmatrix} \quad (16)$$

The covariance of $\mathbf{v}^{\mathrm{CV}}$ is

$$\mathbf{q}^{\mathrm{CV}} = \mathrm{diag}(\sigma_{\ddot{\mathrm{x}}}^2 \quad \sigma_{\ddot{\mathrm{y}}}^2 \quad \sigma_{\mathrm{t}}^2) \quad (17)$$

where $\sigma_{\ddot{x}}^2$ and $\sigma_{\ddot{y}}^2$ are the variances on small target accelerations in the x and y coordinates respectively, and σ_t^2 is the process noise variance on the target time. The covariance of the error in the model (8) is given by

$$\mathbf{Q}^{\mathrm{CV}}(\Delta_k) = \Gamma^{\mathrm{CV}}\mathbf{q}^{\mathrm{CV}}(\Gamma^{\mathrm{CV}})' \quad (18)$$

2) Coordinated Turn Gauss-Helmert model

The GH state transition model for the CT motion is given by

$$\mathbf{g}^{\mathrm{CT}}[\mathbf{x}^{\mathrm{CT}}(t_k), \mathbf{x}^{\mathrm{CT}}(t_{k-1})] + \Gamma^{\mathrm{CT}}\mathbf{v}^{\mathrm{CT}}(t_{k-1}) = \mathbf{0}_6 \quad (19)$$

where

$$\mathbf{g}^{\mathrm{CT}}(\cdot) = \left[g_1^{\mathrm{CT}}(\cdot)\ g_2^{\mathrm{CT}}(\cdot)\ g_3^{\mathrm{CT}}(\cdot)\ g_4^{\mathrm{CT}}(\cdot)\ g_5^{\mathrm{CT}}(\cdot)\ g_6^{\mathrm{CT}}(\cdot)\right]' \quad (20)$$

with

$$\begin{aligned} g_1^{\mathrm{CT}}(\cdot) &= x(t_k) - \left[x(t_{k-1}) + \frac{\sin[\omega(t_{k-1})\Delta_k]}{\omega(t_{k-1})}\dot{x}(t_{k-1}) \right.\\ &\quad \left. - \frac{1-\cos[\omega(t_{k-1})\Delta_k]}{\omega(t_{k-1})}\dot{y}(t_{k-1})\right] && (21)\\ g_2^{\mathrm{CT}}(\cdot) &= y(t_k) - \left[y(t_{k-1}) + \frac{\sin[\omega(t_{k-1})\Delta_k]}{\omega(t_{k-1})}\dot{y}(t_{k-1}) \right.\\ &\quad \left. + \frac{1-\cos[\omega(t_{k-1})\Delta_k]}{\omega(t_{k-1})}\dot{x}(t_{k-1})\right] && (22)\\ g_3^{\mathrm{CT}}(\cdot) &= \dot{x}(t_k) - \{\cos[\omega(t_{k-1})\Delta_k]\dot{x}(t_{k-1}) \\ &\quad - \sin[\omega(t_{k-1})\Delta_k]\dot{y}(t_{k-1})\} && (23)\\ g_4^{\mathrm{CT}}(\cdot) &= \dot{y}(t_k) - \{\sin[\omega(t_{k-1})\Delta_k]\dot{x}(t_{k-1}) \\ &\quad + \cos[\omega(t_{k-1})\Delta_k]\dot{y}(t_{k-1})\} && (24)\\ g_5^{\mathrm{CT}}(\cdot) &= \omega(t_k) - \omega(t_{k-1}) && (25)\\ g_6^{\mathrm{CT}}(\cdot) &= t_k - (t_k^{\mathrm{R}} - \tau_k^{\mathrm{R}}) && (26) \end{aligned}$$

The noise gain matrix Γ^{CT} is given by

$$\Gamma^{\mathrm{CT}} = \begin{bmatrix} \frac{1}{2}(\Delta_k)^2 & 0 & 0 & 0 \\ 0 & \frac{1}{2}(\Delta_k)^2 & 0 & 0 \\ \Delta_k & 0 & 0 & 0 \\ 0 & \Delta_k & 0 & 0 \\ 0 & 0 & \Delta_k & 0 \\ 0 & 0 & 0 & 1 \end{bmatrix} \quad (27)$$

$$\mathbf{q}^{\mathrm{CT}} = \mathrm{diag}(\sigma_{\ddot{x}}^2 \quad \sigma_{\ddot{y}}^2 \quad \sigma_{\omega}^2 \quad \sigma_t^2) \quad (28)$$

where σ_ω^2 is the variance of the Gaussian process noises of ω. The covariance of the error in (19) for the (nearly) CT motion, $\mathbf{Q}^{\mathrm{CT}}(\Delta_k)$, is computed by

$$\mathbf{Q}^{\mathrm{CT}}(\Delta_k) = \Gamma^{\mathrm{CT}}\mathbf{q}^{\mathrm{CT}}(\Gamma^{\mathrm{CT}})' \quad (29)$$

B. Measurement model

The measurement model relates the state at time t_k to the measurement at time t_k^{R}, which is given by

$$\mathbf{z}(t_k^{\mathrm{R}}) = \mathbf{h}[\mathbf{x}(t_k)] + \mathbf{w}(t_k^{\mathrm{R}}) \quad (30)$$

where $\mathbf{w}(t_k^{\mathrm{R}})$ is the measurement noise, and

$$\mathbf{h}(\cdot) = [h_1(\cdot)\ h_2(\cdot)]' \quad (31)$$

with

$$\begin{aligned} h_1(\cdot) &= b(t_k^{\mathrm{R}}) = \tan^{-1}\left[\frac{x(t_k) - x^{\mathrm{R}}}{y(t_k) - y^{\mathrm{R}}}\right] && (32)\\ h_2(\cdot) &= f^{\mathrm{R}}(t_k^{\mathrm{R}}) = f^{\mathrm{T}}(t_k^{\mathrm{T}})\left[1 - \frac{\dot{r}(t_k^{\mathrm{R}})}{c^{\mathrm{P}}}\right] && (33) \end{aligned}$$

The challenge is how to obtain $\dot{r}(t_k^{\mathrm{R}})$ in (33). We know

$$\begin{aligned} r(t_k^{\mathrm{R}}) &= r_k^{\mathrm{T}} + r_k^{\mathrm{R}}\\ &= \sqrt{[x(t_k) - x^{\mathrm{T}}]^2 + [y(t_k) - y^{\mathrm{T}}]^2}\\ &\quad + \sqrt{[x(t_k) - x^{\mathrm{R}}]^2 + [y(t_k) - y^{\mathrm{R}}]^2} && (34) \end{aligned}$$

and

$$\begin{aligned} \dot{r}(t_k^{\mathrm{R}}) &= \frac{d[r(t_k^{\mathrm{R}})]}{d(t_k^{\mathrm{R}})}\\ &= \frac{\dot{x}(t_k)[x(t_k) - x^{\mathrm{T}}] + \dot{y}(t_k)[y(t_k) - y^{\mathrm{T}}]}{r_k^{\mathrm{T}}}\frac{dt_k}{d(t_k^{\mathrm{R}})}\\ &\quad + \frac{\dot{x}(t_k)[x(t_k) - x^{\mathrm{R}}] + \dot{y}(t_k)[y(t_k) - y^{\mathrm{R}}]}{r_k^{\mathrm{R}}}\frac{dt_k}{d(t_k^{\mathrm{R}})} && (35) \end{aligned}$$

When the signal propagation delay is negligible (for example, for a radar signal), one has $t_k = t_k^{\mathrm{R}}$ and

$$\frac{dt_k}{d(t_k^{\mathrm{R}})} = 1 \tag{36}$$

The analytical form of $\dot{r}(t_k^{\mathrm{R}})$ is then

$$\begin{aligned}\dot{r}(t_k^{\mathrm{R}}) &= \frac{\dot{x}(t_k)[x(t_k) - x^{\mathrm{T}}] + \dot{y}(t_k)[y(t_k) - y^{\mathrm{T}}]}{r_k^{\mathrm{T}}} \\ &+ \frac{\dot{x}(t_k)[x(t_k) - x^{\mathrm{R}}] + \dot{y}(t_k)[y(t_k) - y^{\mathrm{R}}]}{r_k^{\mathrm{R}}}\end{aligned} \tag{37}$$

However, the acoustic signal in our problem has significant propagation delay and $t_k \neq t_k^{\mathrm{R}}$. The analytical function

$$t_k = f(t_k^{\mathrm{R}}) \tag{38}$$

is impossible to obtain for a target in CT motion. This causes a major challenge for mapping the state to the measurement. An appropriate filter to cope with this challenge will be developed next.

III. Interacting Multiple Model Unscented Gauss-Helmert Filter with Numerical Jacobian

The IMM estimator [1] is the most commonly used hybrid approach to handle model uncertainty in target tracking. This section describes an IMM-UGHF-NJ filter with the implicit CV and CT models described in Section II and lack of analytical expression for the measurement function.

Similarly to the original IMM estimator, the IMM-UGHF-NJ performs the state estimation in four steps: mixing, mode-matched filtering, mode probabilities updating and final state combination:

1) In the mixing step, the m hypotheses (where m is the the number of models in the filter) at time k-1 expand to m^2 hypotheses using the mixing probabilities based on the mode Markov chain, which is governed by the $m \times m$ mode probability transition matrix Π consisting of the mode transition probabilities, p_{ij}. The m^2 hypotheses are then merged into m hypotheses based on the mixture equations [1].
2) In the mode-matched filtering step, the mixed state estimates are updated by UGHF-NJs (given later) in parallel.
3) The mixing probabilities are obtained, and the updated mode probabilities are computed based on the innovations in the mode-matched UGHF-NJs. The updated mode probabilities together with the mode-conditioned estimated states and covariances are brought to the next step.
4) The final state estimate and its covariance for the current time cycle are computed based on the mixture equations using the latest mode probabilities in the combination step.

Since the states in the CV and CT models described in Section II have different dimensions, the unbiased mixing approach [13] is applied in the IMM filter to increase the CV state from 5 to 6. Before the mixing step, the CV state estimate and its error covariance are augmented with the turn rate information from the CT model.

The IMM-UGHF-NJ differs from the standard IMM in the mode-matched filters, which are UGHF-NJ. The UGHF-NJ handles the implicit GH state transition model and evaluates $f^{\mathrm{R}}(t_k^{\mathrm{R}})$ in the measurement vector (3) numerically. The UGHF-NJ prediction, state-to-measurement mapping and update steps are given in Algorithms 1–3, respectively. In these algorithms, the model superscripts "CV" and "CT" for the states and GH functions are omitted for simplicity.

Algorithm 1 UGHF-NJ prediction

Generate $(2n_{\mathbf{x}} + 1)$ sigma points for $\hat{\mathbf{x}}(t_{k-1})$:

$$[\{\hat{\mathbf{x}}^i(\hat{t}_{k-1}^i)\}, \{w^i\}] = \mathrm{SigPt}[\hat{\mathbf{x}}(\hat{t}_{k-1}), \mathbf{P}(\hat{t}_{k-1}), \kappa]$$

Predict sigma points using Gauss-Newton algo.:

for all $\hat{\mathbf{x}}^i(\hat{t}_{k-1}^i)$, $i \in \{1, \ldots, 2n_{\mathbf{x}} + 1\}$ **do**

$$\mathbf{x}_0 = \hat{\mathbf{x}}^i(\hat{t}_{k-1}^i)$$

$$\breve{\mathbf{x}}^i(\hat{t}_k^i|\hat{t}_{k-1}^i) = \mathrm{GaussN}[\mathbf{g}(\mathbf{x}_1, \mathbf{x}_0)]$$

end for

Regenerate sigma points with process noise:

$$\hat{\mathbf{x}}(\hat{t}_k|\hat{t}_{k-1}) = \sum_{i=1}^{2n_{\mathbf{x}}+1} w^i \breve{\mathbf{x}}^i(\hat{t}_k^i|\hat{t}_{k-1}^i)$$

$$\mathbf{P}(\hat{t}_k|\hat{t}_{k-1}) = \sum_{i=1}^{2n_{\mathbf{x}}+1} w^i \tilde{\mathbf{x}}^i(\hat{t}_k^i|\hat{t}_{k-1}^i)(\tilde{\mathbf{x}}^i(\hat{t}_k^i|\hat{t}_{k-1}^i))' + \mathbf{Q}(\Delta_k)$$

$$[\{\hat{\mathbf{x}}^i(\hat{t}_k^i|\hat{t}_{k-1}^i)\}, \{w^i\}] = \mathrm{SigPt}[\hat{\mathbf{x}}(\hat{t}_k|\hat{t}_{k-1}), \mathbf{P}(\hat{t}_k|\hat{t}_{k-1}), \kappa]$$

where

$$\tilde{\mathbf{x}}^i(\hat{t}_k^i|\hat{t}_{k-1}^i) = \breve{\mathbf{x}}^i(\hat{t}_k^i|\hat{t}_{k-1}^i) - \hat{\mathbf{x}}(\hat{t}_k|\hat{t}_{k-1})$$

κ is a spread scalar of the sigma points.

Algorithm 1 predicts the state $\hat{\mathbf{x}}(\hat{t}_{k-1})$ from time $\hat{t}_{k-1}$ to an unknown target time, t_k, corresponding to the signal reception time t_k^{R}. The relationship between t_k and t_k^{R} is given by the implicit constraint (5). An unscented Gauss-Helmert approach is used for the state prediction with the implicit constraint. Firstly, $2n_{\mathbf{x}} + 1$ sigma points of $\hat{\mathbf{x}}(\hat{t}_{k-1})$ are generated using $\mathrm{SigPt}(\cdot)$ (given in the Appendix), where $n_{\mathbf{x}}$ is the dimension of the state vector. Secondly, each sigma point is predicted to $\hat{t}_k^i$ using the Gauss-Newton algorithm $\mathrm{GaussN}(\cdot)$ (also given in the Appendix) based on the Gauss-Helmert function $\mathbf{g}(\mathbf{x}_1, \mathbf{x}_0)$, where i is the index of the sigma points. The $2n_{\mathbf{x}} + 1$ $\mathrm{GaussN}(\cdot)$ find $\mathbf{x}_1 = \breve{\mathbf{x}}^i(\hat{t}_k^i|\hat{t}_{k-1}^i)$ from $\mathbf{x}_0 = \hat{\mathbf{x}}^i(\hat{t}_{k-1}^i)$ iteratively. Thirdly, the predicted sigma points are re-generated with considering also the process noise (with the approprate larger prediction covariance).

Algorithm 2 maps the predicted state to the measurement space. The challenge here is that we cannot obtain the Doppler shifted frequency $f^{\mathrm{R}}(t_k^{\mathrm{R}})$ in the measurement from the predicted state directly. The range rate $\dot{r}(t_k^{\mathrm{R}})$ in (33) cannot be derived from the bistatic range $r(t_k^{\mathrm{R}})$, which has no analytical form in terms of t_k^{R}. We use an numerical approach, called numerical Jacobian (NJ), to obtain $\dot{r}(t_k^{\mathrm{R}})$ from $r(t_k^{\mathrm{R}})$. It is known that the slope of the tangent line is the derivative of a

Algorithm 2 UGHF-NJ mapping the predicted state to measurement

$[\{t_k^{\mathrm{R},j}\},\{w^j\}] = \mathrm{SigPt}[t_k^{\mathrm{R}}, \sigma_{t_k^{\mathrm{R}}}, \kappa]$
for all $\hat{\mathbf{x}}^i(\hat{t}_k^i|\hat{t}_{k-1}^i)$, $i \in \{1,\ldots,2n_{\mathbf{x}}+1\}$ **do**
  $\mathbf{x}_0 = \hat{\mathbf{x}}^i(\hat{t}_k^i|\hat{t}_{k-1}^i)$
  for $j = 1:3$ **do**
    $\hat{\mathbf{x}}^{i,j}(\hat{t}_k^j|\hat{t}_{k-1}^i) = \mathrm{GaussN}\left[\mathbf{g}(\mathbf{x}_1,\mathbf{x}_0)|_{t_k^{\mathrm{R}}=t_k^{\mathrm{R},j}}\right]$
    $\hat{r}^{i,j}(t_k^{\mathrm{R}}) \leftarrow \hat{\mathbf{x}}^{i,j}(\hat{t}_k^j|\hat{t}_{k-1}^i)$
  end for
  $\hat{\dot{r}}^i(t_k^{\mathrm{R}}) = \mathrm{NJ}[\{t_k^{\mathrm{R},j}\},\{\hat{r}^{i,j}(t_k^{\mathrm{R}})\},\{w^j\}]$
  $\hat{f}^{\mathrm{R},i}(t_k^{\mathrm{R}}) \leftarrow$ using (33)
  $\hat{b}^i(t_k^{\mathrm{R}}) \leftarrow$ using (32)
  $\mathbf{z}^i(t_k^{\mathrm{R}}) = [\hat{b}^i(t_k^{\mathrm{R}})\ \hat{f}^{\mathrm{R},i}(t_k^{\mathrm{R}})]'$
end for
$\hat{\mathbf{z}}(t_k^{\mathrm{R}}) = \sum_{i=1}^{2n_{\mathbf{x}}+1} w^i \hat{\mathbf{z}}^i(t_k^{\mathrm{R}})$

nonlinear function at a point of interest. The principle of the $\mathrm{NJ}(\cdot)$ (given in the Appendix) is to find the best linear fit to a nonlinear function based on a few weighted points around the point of interest. If we can provide these weighted points around $[t_k^{\mathrm{R}}, r(t_k^{\mathrm{R}})]$, its derivative $\dot{r}(t_k^{\mathrm{R}})$ can then be computed using $\mathrm{NJ}(\cdot)$. Firstly, we generate the reception time set around t_k^{R} using $\mathrm{SigPt}(\cdot)$, i.e.,

$$\{t_k^{\mathrm{R},j}\} = \{t_k^{\mathrm{R}}, t_k^{\mathrm{R}} - \sigma_{t_k^{\mathrm{R}}}, t_k^{\mathrm{R}} + \sigma_{t_k^{\mathrm{R}}}\} \quad j = 1,2,3 \tag{39}$$

where $\sigma_{t_k^{\mathrm{R}}}$ is a very small shift from t_k^{R}. Its weight set is $\{w^j\}$. Secondly, we use $\mathrm{GaussN}(\cdot)$ to obtain the predicted state set $\{\hat{\mathbf{x}}^{i,j}(\hat{t}_k|\hat{t}_{k-1})\}$ corresponding to the reception time set $\{t_k^{\mathrm{R},j}\}$ for the ith sigma point of the predicted state (obtained from Algorithm 1). The bistatic range can then be computed using (34). The set of bistatic ranges corresponding to $\{t_k^{\mathrm{R},j}\}$ for the ith sigma point of the predicted state is

$$\{\hat{r}^{i,j}(t_k^{\mathrm{R}})\} = \{\hat{r}^i(t_k^{\mathrm{R}}), \hat{r}^i(t_k^{\mathrm{R}} - \sigma_{t_k^{\mathrm{R}}}), \hat{r}^i(t_k^{\mathrm{R}} + \sigma_{t_k^{\mathrm{R}}})\} \quad j = 1,2,3 \tag{40}$$

Thirdly, we use these two sets, $\{t_k^{\mathrm{R},j}\}$ and $\{\hat{r}^{i,j}(t_k^{\mathrm{R}})\}$, which form three points around $[t_k^{\mathrm{R}}, \hat{r}^i(t_k^{\mathrm{R}})]$ to evaluate the range rate $\hat{\dot{r}}^i(t_k^{\mathrm{R}})$ using $\mathrm{NJ}(\cdot)$. Once $\hat{\dot{r}}^i(t_k^{\mathrm{R}})$ is obtained, $f^{\mathrm{R},i}(t_k^{\mathrm{R}})$ can be computed using (33), and the predicted measurement $\mathbf{z}^i(t_k^{\mathrm{R}})$ follows.

Algorithm 3 updates the predicted state based on the measurment $\mathbf{z}(t_k^{\mathrm{R}})$. This step is the same as the conventional UKF.

IV. Simulation Results

The IMM-UGHF-NJ is tested by simulated data in this section. The simulated scenarios are shown in Fig. 3. Three targets move in CV-CT-CV motion with different speeds 30m/s, 20m/s and 10m/s, respectively. All three targets have two CV legs linked by a CT arc. The durations of the first CV, CT and the second CV are 130s, 60s and 90s, respectively. The CT arc is a 120° right turn with turn rate 2°/s. The transmitter and receiver are located at (-3500m,0m) and (3500m,0m), respectively. The transmitter emits a CW signal with frequency 1000Hz. The

Algorithm 3 UGHF-NJ update

$\hat{\mathbf{x}}(\hat{t}_k) = \hat{\mathbf{x}}(\hat{t}_k|\hat{t}_{k-1}) + \mathbf{K}_k\nu(t_k^{\mathrm{R}})$
$\mathbf{P}(\hat{t}_k) = \mathbf{P}(\hat{t}_k|\hat{t}_{k-1}) - \mathbf{K}_k\mathbf{S}(t_k^{\mathrm{R}})\mathbf{K}_k'$
where
  $\nu(t_k^{\mathrm{R}}) = \mathbf{z}(t_k^{\mathrm{R}}) - \hat{\mathbf{z}}(t_k^{\mathrm{R}})$
  $\mathbf{K}_k = \mathbf{P}_{xz}\mathbf{S}(t_k^{\mathrm{R}})^{-1}$
  $\mathbf{S}(t_k^{\mathrm{R}}) = \mathbf{R} + \mathbf{P}_{zz}$
  $\mathbf{P}_{xz} = \sum_{i=1}^{2n_{\mathbf{x}}+1} w^i \tilde{\mathbf{x}}^i(\hat{t}_k^i|\hat{t}_{k-1}^i)\tilde{\mathbf{z}}^i(t_k^{\mathrm{R}})'$
  $\mathbf{P}_{zz} = \sum_{i=1}^{2n_{\mathbf{x}}+1} w^i[\tilde{\mathbf{z}}^i(t_k^{\mathrm{R}})\tilde{\mathbf{z}}^i(t_k^{\mathrm{R}})']$
  $\tilde{\mathbf{z}}^i(t_k^{\mathrm{R}}) = \hat{\mathbf{z}}^i(t_k^{\mathrm{R}}) - \hat{\mathbf{z}}(t_k^{\mathrm{R}})$
  $\tilde{\mathbf{x}}^i(\hat{t}_k^i|\hat{t}_{k-1}^i) = \hat{\mathbf{x}}^i(\hat{t}_k^i|\hat{t}_{k-1}^i) - \hat{\mathbf{x}}(\hat{t}_k|\hat{t}_{k-1})$

sampling interval of the receiver is $T = 1$s. The measurement errors of bearing and Doppler shifted frequency at receiver are assumed Gaussian with standard deviations $\sigma_b = 1^{\circ}$ and $\sigma_f = 0.25$Hz, respectively. The sound propagation speed in water is $c^{\mathrm{p}} = 1484$m/s.

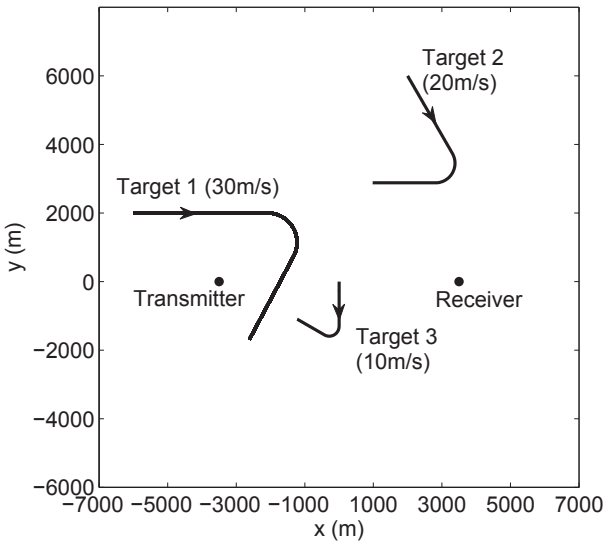

Fig. 3. Test scenarios.

The following two algorithms are used in testing:

- IMM-UKF: The mode-matched filters are UKF. They estimate target position and velocity only. The propagation delay is not taken into consideration at all. The Doppler shifted frequency in the measurement model is based on (37) which is commonly used in multistatic radar tracking system. The target times are the signal reception times by the receiver.
- IMM-UGHF-NJ: This is the new algorithm proposed in this paper. The propagation delay is taken into consideration in the state estimation, and the target

times attached to the target trajectory are estimated from multiple UGHF-NJs.

One CV model and one CT model are used in the two IMM estimators. The initial mode probabilities for both models are 0.5. The probability transition matrix Π is

$$\Pi = \begin{bmatrix} 0.95 & 0.05 \\ 0.05 & 0.95 \end{bmatrix} \quad (41)$$

The measurement error covariance $\mathbf{R}$ is

$$\mathbf{R} = \mathrm{diag}[(1^{\mathrm{o}})^2 \ (0.25\mathrm{Hz})^2] \quad (42)$$

The process noise covariances $\mathbf{q}^{\mathrm{CV}}$ and $\mathbf{q}^{\mathrm{CT}}$ in the UGHF-NJs are, respectively,

$$\mathbf{q}^{\mathrm{CV}} = \mathrm{diag}[(0.1\mathrm{m/s}^2)^2 \ (0.1\mathrm{m/s}^2)^2 \ (0.1\mathrm{s})^2] \quad (43)$$

$$\mathbf{q}^{\mathrm{CT}} = \mathrm{diag}[(0.1\mathrm{m/s}^2)^2 \ (0.1\mathrm{m/s}^2)^2 \ (0.1^{\mathrm{o}}/\mathrm{s})^2 \ (0.1\mathrm{s})^2] \quad (44)$$

κ is set to 1 in all $\mathrm{SigPt}(\cdot)$, and $\sigma_{t_k^{\mathrm{R}}}$ is set to 0.1s in Algorithm 2.

The initial state estimates are

$$\hat{\mathbf{x}}^{\mathrm{CV}}(t_0) = [\hat{r}_0 \sin b_0 \ \hat{r}_0 \cos b_0 \ 0 \ 0 \ \hat{t}_0]' \quad (45)$$

$$\hat{\mathbf{x}}^{\mathrm{CT}}(t_0) = [\hat{r}_0 \sin b_0 \ \hat{r}_0 \cos b_0 \ 0 \ 0 \ 0.1^{\mathrm{o}}/\mathrm{s} \ \hat{\mathrm{t}}_0]' \quad (46)$$

where

$$\begin{aligned} \hat{r}_0 &\sim \mathcal{N}(r_0^{\mathrm{R}}, \sigma_r^2) && (47) \\ b_0 &= b(t_0^{\mathrm{R}}) && (48) \\ \hat{t}_0 &= t_0^{\mathrm{R}} - \hat{r}_0/c^{\mathrm{p}} && (49) \end{aligned}$$

with r_0^{R} is the true value of the range from the target at time t_0 to the receiver at time t_0^{R}, $\sigma_r = 600m$, and $b(t_0^{\mathrm{R}})$ is the measured bearing at time t_0^{R}. The initial state error covariances for the two models are

$$\mathbf{P}^{\mathrm{CV}}(t_0) = \begin{bmatrix} P_{xx} & P_{xy} & 0 & 0 & 0 \\ P_{yx} & P_{yy} & 0 & 0 & 0 \\ 0 & 0 & 400 & 0 & 0 \\ 0 & 0 & 0 & 400 & 0 \\ 0 & 0 & 0 & 0 & (\sigma_r/c^{\mathrm{p}})^2 \end{bmatrix} \quad (50)$$

$$\mathbf{P}^{\mathrm{CT}}(t_0) = \begin{bmatrix} P_{xx} & P_{xy} & 0 & 0 & 0 & 0 \\ P_{yx} & P_{yy} & 0 & 0 & 0 & 0 \\ 0 & 0 & 400 & 0 & 0 & 0 \\ 0 & 0 & 0 & 400 & 0 & 0 \\ 0 & 0 & 0 & 0 & (2^{\mathrm{o}}/s)^2 & 0 \\ 0 & 0 & 0 & 0 & 0 & (\sigma_r/c^{\mathrm{p}})^2 \end{bmatrix} \quad (51)$$

where

$$\begin{aligned} P_{xx} &= (\hat{r}_0\sigma_b \cos b_0)^2 + (\sigma_r \sin b_0)^2 && (52) \\ P_{yy} &= (\hat{r}_0\sigma_b \sin b_0)^2 + (\sigma_r \cos b_0)^2 && (53) \\ P_{xy} &= P_{yx} = (\sigma_r^2 - \hat{r}_0^2\sigma_b^2) \sin b_0 \cos b_0 && (54) \end{aligned}$$

The simulation results present the root mean square errors (RMSE) of the estimated target positions obtained from 100 Monte Carlo runs. The estimated position error at time $\hat{t}_k$ is computed by

$$\mathrm{pos}^{\mathrm{err}}(\hat{t}_k) = \sqrt{[\hat{x}(\hat{t}_k) - x(\hat{t}_k)]^2 + [\hat{y}(\hat{t}_k) - y(\hat{t}_k)]^2} \quad (55)$$

where $\hat{x}(\hat{t}_k)$ and $\hat{y}(\hat{t}_k)$ are the estimated target positions in the x and y coordinates respectively, $x(\hat{t}_k)$ and $y(\hat{t}_k)$ are the true target positions in the x and y coordinates respectively, and $\hat{t}_k$ is the estimated target time in estimation cycle k.

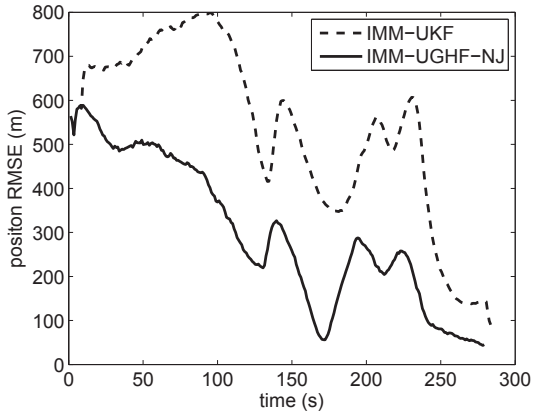

Fig. 4. Position estimate RMSEs versus time for target 1 with speed=30m/s.

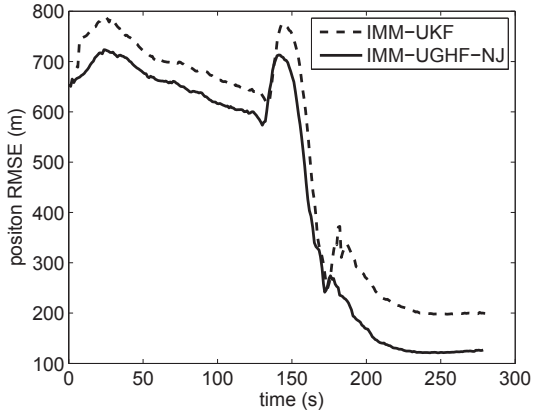

Fig. 5. Position estimate RMSEs versus time for target 2 with speed=20m/s.

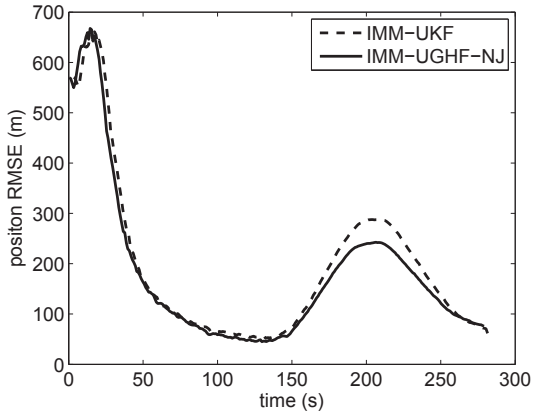

Fig. 6. Position estimate RMSEs versus time for target 3 with speed=10m/s.

Figs. 4–6 show the position RMSE versus time of the two algorithms for the three simulated targets. The averages

of position and speed RMSEs per run are summarized in Tables I and II. It can be seen that the IMM-UGHF-NJ outperforms the IMM-UKF for all the three targets. The accuracy improvement is target speed dependent. For a fast target there is more improvement than for a slow one. This is because that estimation error of the IMM-UKF relates to the target speed and propagation delay τ_k^{R} (details can be found in Section V-C, [10]). From the results we can say that the estimation error without considering propagation delay for fast targets, such as a speed boat or torpedo, is significant.

TABLE I. AVERAGES OF POSITION RMSE PER RUN

Target	IMM-UKF	IMM-UGHF-NJ
1 (30m/s)	571.7m	339.6m
2 (20m/s)	556.8m	509.4m
3 (10m/s)	246.9m	237.8m

TABLE II. AVERAGES OF SPEED RMSE PER RUN

Target	IMM-UKF	IMM-UGHF-NJ
1 (30m/s)	8.9m/s	5.6m/s
2 (20m/s)	4.7m/s	4.3m/s
3 (10m/s)	4.9m/s	4.4m/s

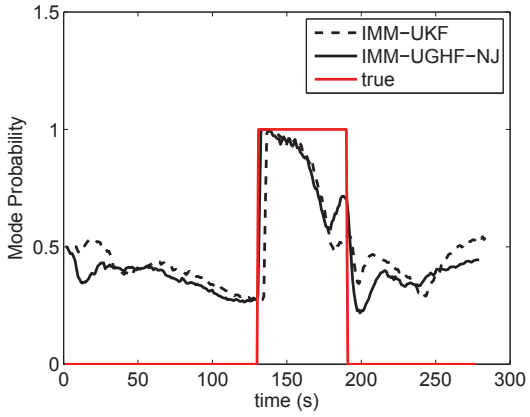

Fig. 7. Mode probability of CT model versus time for target 1 (speed=30m/s).

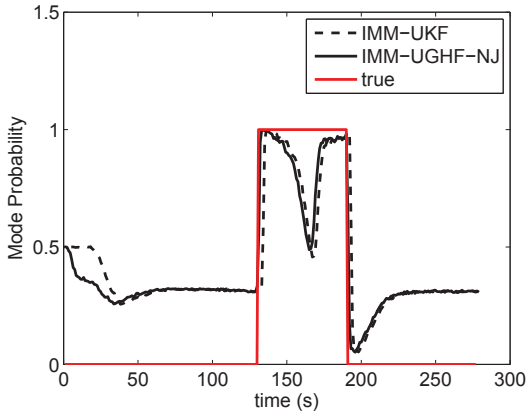

Fig. 8. Mode probability of CT model versus time for target 2 (speed=20m/s).

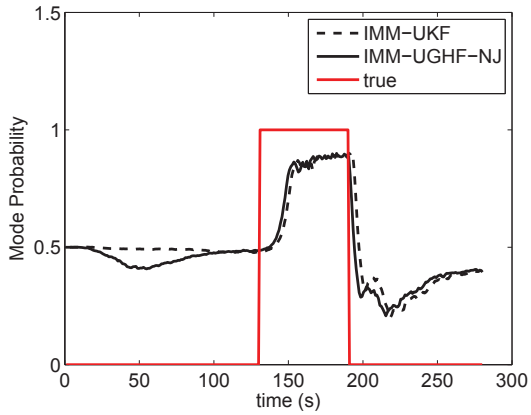

Fig. 9. Mode probability of CT model versus time for target 3 (speed=10m/s).

The mode probability of the two IMM filters is also investigated. Figs. 7–9 show the mode probability of CT model versus time for the three targets, respectively. It can be seen that the mode probabilities of CT for both filters increase when target is maneuvering. The IMM-UGHF-NJ reacts slightly faster than the IMM-UKF. However, the mode probability does not match the ground truth very well when the target is in CV motion. This is because that the turn rate ω can adapt to a small value when the target is in CV motion. This leads to target motion patterns that are marginally observable from bearing and Doppler frequency measurements. We also observed that the mode probability during CT is imperfect. It is not steady for targets 1 and 2 (shown in Figs 7 and 8), and has slow adaptation for target 3 (shown in Fig 9). This is because the turn rate ω cannot adapt to the correct value, and leads to target motion patterns marginally observable. Further study on this issue has been conducted [12].

V. CONCLUSIONS

This paper developed the IMM-UGHF-NJ filter to track maneuvering target using bistatic CW-CAS in the presence of propagation delay. The IMM-UGHF-NJ can overcome two challenges of this tracking problem, namely, the implicit state transition model and absence of analytical expression of the Doppler shifted frequency in the measurement model. Simulation tests were conducted on targets with different speeds. Results show that the IMM-UGHF-NJ outperforms the IMM-UKF which does not take the propagation delay into consideration. It is also found that the estimate accuracy improvement of the IMM-UGHF-NJ over the IMM-UKF is more significant for a higher speed target. This is because the effect of the propagation delay is speed dependent. A faster target (such as a speed boat or a torpedo) needs an appropriate filter (IMM-UGHF-NJ) to handle the propagation delay.

APPENDIX

The three algorithms $\mathrm{SigPt}(\cdot)$, $\mathrm{GaussN}(\cdot)$ and $\mathrm{NJ}(\cdot)$ used in IMM-UGHF-NJ are given next.

a) $\mathrm{SigPt}(\cdot)$ generates the sigma points for a random

variable $\mathbf{x}$ with covariance $\mathbf{P_x}$ [5].

$$[\mathbf{x}^i, w^i] = \mathrm{SigPt}(\mathbf{x}, \mathbf{P_x}, \kappa) \qquad i = 1, \ldots, 2n_\mathbf{x}+1 \tag{56}$$

where

$$\begin{aligned} \mathbf{x}^1 &= \mathbf{x} && (57)\\ \mathbf{x}^i &= \mathbf{x} + \left[\sqrt{(n_\mathbf{x}+\kappa)\mathbf{P_x}}\right]_{i-1} \\ & && i = 2, \cdots, n_\mathbf{x}+1 \quad (58)\\ \mathbf{x}^i &= \mathbf{x} - \left[\sqrt{(n_\mathbf{x}+\kappa)\mathbf{P_x}}\right]_{i-n_\mathbf{x}-1} \\ & && i = n_\mathbf{x}+2, \cdots, 2n_\mathbf{x}+1 \quad (59) \end{aligned}$$

$$\begin{aligned} w_0 &= \frac{\kappa}{n_\mathbf{x}+\kappa} && i = 1 \quad (60)\\ w_i &= \frac{1}{2(n_\mathbf{x}+\kappa)} && i = 2, \cdots, 2n_\mathbf{x}+1 \quad (61) \end{aligned}$$

where $n_\mathbf{x}$ is the dimension of $\mathbf{x}$, $\left[\sqrt{(n_\mathbf{x}+\kappa)\mathbf{P_x}}\right]_{i^*}$ indicates the i^*th column of the matrix $[\cdot]$, and κ is a scalar that determines the spread of sigma points.

b) $\mathrm{GaussN}(\cdot)$ is a Gauss-Newton algorithm to obtain the solution of an implicit equation $\mathbf{g}(\cdot) = \mathbf{0}$ iteratively [9][10] and yields

$$\hat{\mathbf{x}}_1 = \mathrm{GaussN}[\mathbf{g}(\mathbf{x}_1, \mathbf{x}_0)] \tag{62}$$

where $\mathbf{x}_0$ is known. The iteration procedure is

$$\hat{\mathbf{x}}_1^{j+1} = \hat{\mathbf{x}}_1^j - (\mathbf{A}^j)^{-1}\mathbf{g}(\hat{\mathbf{x}}_1^j, \mathbf{x}_0) \tag{63}$$

where j is the iteration index, $\mathbf{A}^j$ is the Jacobian matrix defined by

$$\mathbf{A}^j = \frac{\partial \mathbf{g}[(\hat{\mathbf{x}}_1^j, \mathbf{x}_0)]}{\partial \hat{\mathbf{x}}_1^j} \tag{64}$$

c) $\mathrm{NJ}(\cdot)$ calculates the Jacobian (or derivative) $\mathbf{H}$ of a function

$$\mathbf{z} = \mathbf{h}(\mathbf{x}) \tag{65}$$

at a point of interest $\mathbf{x}_0$ numerically [6][11][7]. There is no analytical form for $\mathbf{h}(\cdot)$, but $\mathbf{z}$ can be obtained through numerical method from a given $\mathbf{x}$. The Jacobian is

$$\mathbf{H} = \mathrm{NJ}[\{\mathbf{x}^i\}, \{\mathbf{z}^i\}, \{w^i\}] \tag{66}$$

where $\{\mathbf{x}^i\}$ is the sigma point set around $\mathbf{x}_0$ generated from a very small covariance, $\{\mathbf{z}^i\}$ is its corresponding set after transformation and $\{w^i\}$ is the set of weights. The NJ is implementing through the following steps:

1) Form the sigma point set

$$\bar{\mathbf{X}} = \begin{bmatrix} \mathbf{x}^1 & \mathbf{x}^2 & \cdots & \mathbf{x}^{2n_\mathbf{x}+1} \\ 1 & 1 & \cdots & 1 \end{bmatrix} - \begin{bmatrix} \mathbf{x}^1 \\ 0 \end{bmatrix} \tag{67}$$

$$\mathbf{Z} = \begin{bmatrix} \bar{\mathbf{z}}^1 \\ \bar{\mathbf{z}}^2 \\ \vdots \\ \bar{\mathbf{z}}^l \end{bmatrix} = \begin{bmatrix} \mathbf{z}^1 & \mathbf{z}^2 & \cdots & \mathbf{z}^{2n_\mathbf{x}+1} \end{bmatrix} \tag{68}$$

where $\mathbf{x}^1 = \mathbf{x}_0$, and l is the dimension of $\mathbf{z}$.

2) Estimate $\mathbf{H}$ using the weighted least squares (WLS) algorithm

$$\mathbf{a}^j = (\bar{\mathbf{X}}\mathbf{W}\bar{\mathbf{X}}')^{-1}\bar{\mathbf{X}}\mathbf{W}(\bar{\mathbf{z}}^j)' \tag{69}$$

$$\hat{\bar{\mathbf{H}}} = \begin{bmatrix} \mathbf{a}^1 & \mathbf{a}^2 & \cdots & \mathbf{a}^l \end{bmatrix}' \tag{70}$$

$$\hat{\mathbf{H}} = \hat{\bar{\mathbf{H}}}(1 : l, 1 : n_\mathbf{x}) \tag{71}$$

where $\mathbf{W} = \mathrm{diag}(\{w^i\})$, $j \in \{1, \ldots, l\}$, and $\hat{\mathbf{H}}$ is $\hat{\bar{\mathbf{H}}}$ without the last column.

REFERENCES

[1] Bar-Shalom, Y., Willett, P.K. and Tian, X., *Tracking and Data Fusion: A Handbook of Algorithms*, YBS Publishing, 2011.

[2] DeFerrari H.A., "The Application of m-Sequences to Bi-static Active Sonar", *Journal of the Acoustical Society of America*, 114(4):2399-2400, 2003.

[3] Grimmett, D., Wakayama, C., "Multistatic Tracking for Continous Active Sonar using Doppler-Bearing Measurements", *Proc. 16th International Conference on Information Fusion*, Istanbul, Turkey, Jul. 2013.

[4] Jauffret, C., Pérez, A.-C., Blanc-Benon, P., Tanguy, H., "Doppler-only Target Motion Analysis in a High Duty Cycle Sonar System", *Proc. 19th International Conference on Information Fusion*, Heidelburg, Germany, Jul. 2016.

[5] Julier, S.J., and Uhlmann, J.K., "A new extension of the Kalman filter to nonlinear systems", *Proceedings of AeroSense: The 11th International Symposium on Aerospace/Defence Sensing, Simulation and Controls*, Apr. 1997.

[6] Xiong, Y.B., Zhong, X.H., and Yang, R., "The linear fitting Kalman filter for nonlinear tracking", *Proceedings of the 5th Asia-Pacific Conference on Synthetic Aperture Radar*, Singapore, Sep. 2015.

[7] Xiong, Y.B., and Zhong, X.H., "Linear fitting Kalman filter", *IET Signal Processing*, 10(4):404–412, Jun. 2016.

[8] Yang, T.E.,"Acoustic Dopplergram for Intruder Defense", *Proceedings of IEEE Oceans 2007*, Vancouver, BC, Canada, Sep. 2007.

[9] Yang, R., Bar-Shalom, Y., Huang, J.H. and Ng, G.W., "Interacting multiple model unscented Gauss-Helmert filter for bearings-only tracking with state-dependent propagation delay", *Proc. 17th International Conference on Information Fusion*, Salamanca, Spain, Jul. 2014.

[10] Yang, R., Bar-Shalom, Y., Huang, J.H. and Ng, G.W., "UGHF for acoustic tracking with state-dependent propagation delay", *IEEE Transactions on Aerospace and Electronic Systems*, 51(3):1747–1761, Aug. 2015.

[11] Yang, R., and Bar-Shalom, Y. "Comparison of altitude estimation using 2D and 3D radars over spherical Earth", *Proceedings of IEEE Aerospace Conference 2016*, Big Sky, MT, USA, Mar. 2016.

[12] Yang, R., Bar-Shalom, Y., Jauffret, C., Pérez, A.-C., and Ng G.W. "Maneuvering target tracking using continuous wave bistatic sonar with propagation delay", to appear in *Journal of Advances in Information Fusion,* 2018.

[13] Yuan, T., Bar-Shalom, Y., Willett, P., Mozeson, E., Pollak, S. and Hardiman D., "A multiple IMM estimation approach with unbiased mixing for thrusting projectiles", *IEEE Transactions on Aerospace and Electronic Systems*, 48(4):3250-3267, Oct. 2012.